JET-P(95)43

Sawtooth Heat Pulse Propagation in Tokamaks: Ballistic Response and Fourier Analysis

F De Luca[1], N Deliyanakis, M Erba, P Galli[1], G Gorini[1], A Jacchia[2], P Mantica[2], L Porte.

JET Joint Undertaking, Abingdon, Oxfordshire, OX14 3EA, UK.

[1] Dipartimento di Fisica, Universita degli Studi di Milano, 20133 Milano, Italy.

[2] Istituto di Fisica del Plasma, Associazione EURATOM–ENEA–CNR, 20133 Milano, Italy.

Preprint of a Paper to be submitted for publication in Nuclear Fusion

September 1995

Abstract

Fourier analysis is proposed as a tool for the recognition of non-diffusive features of heat pulse propagation in fusion plasmas. Application to a simulated ballistic sawtooth heat pulse shows that Fourier analysis can identify the plasma region (often well beyond the mixing radius) where the heat pulse is diffusive. In this region the initial temperature perturbation, as recorded by a diagnostic with moderate (≈1 kHz) time resolution, is negligible. Fourier analysis of an example of JET sawtooth heat pulse diagnosed with the new ECE heterodyne diagnostics is consistent with the results from the simulated ballistic heat pulse. It cannot however be used as an evidence of a ballistic effect due to the limited diagnostic time resolution. When both the perturbed (χ_e^P) and the power balance (χ_e^{PB}) diffusivity can be determined reliably in recent JET sawtoothing plasmas, their ratio is $\chi_e^P/\chi_e^{PB}\approx 2\text{-}4$ in agreement with previous results.

1. Introduction

Sawtooth heat pulse propagation has been widely used to investigate the transport of thermal energy in tokamak plasmas. The standard approach for the interpretation of sawtooth heat pulses is to assume that the process is diffusive. Different methods of analysis can then be applied to determine a "perturbative" electron heat diffusivity, χ_e^P, from heat pulse data [1]. The ratio of χ_e^P with the electron heat diffusivity from steady-state power balance analysis, χ_e^{PB}, is usually observed to lie in the range $1<\chi_e^P/\chi_e^{PB}<5$, and can be explained by a non-linear (or offset-linear) dependence of the heat flux on the temperature gradient. This result is confirmed by other perturbative heat transport studies including power modulation and pellet injection experiments.

Unlike other perturbation techniques, the temperature perturbation following a sawtooth crash is the result of an MHD instability. This instability is generally observed to be very fast (timescale $\tau_{ST}\approx 100$ μs) and localised within the so-called mixing radius (r_{mix}). The assumption that the plasma outside r_{mix} is not affected by the MHD instability is essential in order to treat the heat pulse as diffusive in that region. Doubts on the validity of this assumption have arisen following the observation of the so-called ballistic effect in TFTR sawtooth heat pulses [2]. The effect consists in an anomaly of the heat pulse propagation outside r_{mix} as observed with fast (200 kHz) measurements of the electron temperature. This has been modelled in terms of a strong enhancement of the heat diffusivity extending outside r_{mix} on a timescale $\tau_b\approx 1$ ms. There ensues a different picture of the sawtooth event, with two phases: the crash phase, occurring on a fast time scale τ_{ST} and confined within r_{mix}; and the ballistic phase, occurring on a slower time scale τ_b (still much faster than heat pulse propagation times) and characterised by enhanced transport over a significant portion of the plasma volume extending outside r_{mix}.

The possibility to derive a meaningful value of χ_e^P from sawtooth heat pulse propagation studies depends on the strength of the ballistic effect. Unfortunately, the need for very fast measurements of the electron temperature has so far limited the investigation of the two phases of the sawtooth crash to the TFTR and TEXTOR tokamaks (in the latter case [3],

too, anomalies in the heat pulse propagation have been detected, but their explanation in terms of ballistic heat pulse propagation is not conclusive). It is therefore of interest to see if any method exists for detecting anomalies in the sawtoth heat pulse propagation when measured with diagnostics with moderate (1-10 kHz) time resolution. The observation of non-diffusive features in the heat pulse is not in itself a proof of the ballistic model for the sawtooth crash. On the other hand, a proof of the diffusive nature of the heat pulse outside a certain radius allows for standard heat pulse propagation studies to be made in that plasma region without knowing the detailed dynamics of the sawtooth cash.

In order to look for non-diffusive features of sawtooth heat pulses in JET, Fourier analysis was applied to JET data in [4]. The Fourier method is very sensitive to non-diffusive features in the heat pulses, especially during the initial rise of the pulse when a ballistic contribution may be present. Fourier analysis is also more sensitive to noise in the data, which limited the applicability of the technique. The availability of a new ECE electron temperature diagnostic in JET, delivering data with better spatial resolution and s/n ratio than previously available, provides an opportunity for a more detailed analysis of heat pulse propagation in JET.

The purpose of this paper is to illustrate how Fourier analysis of heat pulse propagation can be used to find non-diffusive features in the pulses. This is done by taking a simulated ballistic heat pulse as an example. The results of the simulation are then compared with a recent example of JET ST heat pulses diagnosed with the new ECE heterodyne diagnostic.

2. Simulation of a ballistic heat pulse

Starting from the electron energy conservation equation

$$\frac{3}{2} n_{e0} \dot{T}_e - \nabla \cdot \left(n_{e0} \chi_e \nabla T_e \right) = p_e \qquad (1)$$

the equation describing the time evolution of a sawtooth heat pulse is obtained by subtraction of the steady-state power balance

$$-\nabla \cdot \left(n_{e0} \chi_{e0} \nabla T_{e0} \right) = p_{e0} \cdot \qquad (2)$$

The difference equation can be written in terms of the perturbed quantities $\tilde{T}_e=T_e-T_{e0}$, $\tilde{p}_e=p_e-p_{e0}$ and $\tilde{\chi}_e=\chi_e-\chi_{e0}$ as

$$\frac{3}{2}n_{e0}\dot{\tilde{T}}_e-\nabla\cdot\left[n_{e0}\left(\chi_e\nabla\tilde{T}_e+\tilde{\chi}_e\nabla T_{e0}\right)\right]=\tilde{p}_e \qquad (3)$$

In these equations, $T_e(r,t)$ and $n_e(r)$ are the electron temperature and density, respectively, p_e is the electron energy source density, and χ_e is the electron diffusivity. The subscript 0 refers to equilibrium quantities; in particular, χ_{e0} is the power balance diffusivity (commonly denoted as χ_e^{PB}). For simplicity the heat flux is assumed to be diffusive (i.e., convection is neglected). Furthermore, it is assumed that the density perturbation is negligible.

In order to further simplify Eq.3, some assumption on χ_e must be made. According to the "local transport paradigm" [5] χ_e is normally assumed to be a function of local macroscopic plasma parameters such as T_e and ∇T_e. By further assuming that the temperature perturbation is small (i.e., $\tilde{T}_e/T_{e0}<<1$) Eq.3 can be linearised in $\tilde{T}_e$ and $\nabla\tilde{T}_e$. Linearization of χ_e and p_e in $\tilde{T}_e$ yields convective and damping (energy sink) terms. These terms normally play a minor role in the heat pulse propagation and will be disregarded here. Linearization of χ_e in $\nabla\tilde{T}_e$ yields the usual equation for sawtooth heat pulse propagation

$$\frac{3}{2}n_{e0}\dot{\tilde{T}}_e-\nabla\cdot\left[n_{e0}\left(\chi_e^p\nabla\tilde{T}_e\right)\right]=0 \qquad (4)$$

where $\chi_e^p=\chi_{e0}+\frac{\partial\chi_{e0}}{\partial\nabla T_e}\nabla T_{e0}$ is the perturbed heat diffusivity and terms of order $(\nabla\tilde{T}_e)^2$ have been neglected.

The assumption that χ_e be a function of local macroscopic plasma parameters is not valid in the case of a ballistic heat pulse. The enhancement of χ_e following the sawtooth crash can be modelled heuristically by assuming that χ_e is enhanced by a coefficient which is an explicit function of time (t) and radius (r):

$$\chi_e=\gamma(t,r)\chi_{e0} \qquad (5)$$

In this expression, χ_{e0} can be a function of local plasma parameters (notably ∇T_e), while the explicit time-dependence of χ_e violates the local transport paradigm. In order to derive a diffusion equation for a ballistic heat pulse, one has to go back to Eq.3 and replace χ_e and $\tilde{\chi}_e$ with their expressions as prescribed by Eq.5. The resulting equation can further be linearised in $\nabla\tilde{T}_e$ to yield

$$\frac{3}{2} n_{e0} \dot{\tilde{T}}_e - \nabla \cdot \left[n_{e0} \gamma(r,t) \chi_c^p \nabla \tilde{T}_e \right] = \nabla \cdot \{ [\gamma(r,t) - 1] n_{e0} \chi_{c0} \nabla T_{e0} \} \quad (6)$$

Apart from the enhancement of $\chi_e{}^p$ on the left hand side, the ballistic effect contributes an additional (time dependent) source term to the right hand side.

Examples of simulated ballistic heat pulses can be obtained by solving Eq.6 numerically after having specified the functional expressions of $\gamma(r,t)$, $\chi_e{}^p(r)$, $\chi_{e0}(r)$, $n_{e0}(r)$ and $T_{e0}(r)$, as well as the initial and boundary conditions for $\tilde{T}_e$. The simulation of Fig.1 was obtained with the following specifications:

a) Equilibrium quantities:

$$n_{e0}(r) = n_0 \left[1 - \left(\frac{r}{a} \right)^2 \right] + n_a \quad (7)$$

$$T_{e0}(r) = T_0 \left[1 - \left(\frac{r}{a} \right)^2 \right]^4 \quad (8)$$

$$\chi_{e0} = \chi_0 + (\chi_1 - \chi_0) \left(\frac{r}{a} \right)^2 \quad (9)$$

where the numerical values $n_0=3.46 \cdot 10^{19}$ m^{-3}, $n_a=0.12 \cdot 10^{19}$ m^{-3}, $T_0=7$ keV, $\chi_0=0.5$ m^2/s, $\chi_1=2$ m^2/s have been used. The plasma minor radius is a=1 m.

b) Perturbation quantities:

$$\chi_e{}^p = \chi_{e0} \quad (10)$$

$$\gamma(r,t) = [1 + \delta \exp(-t/\tau_b - k\, r^2)] \quad (11)$$

with $\delta=35$, $\tau_b=1$ ms and $k = 16$ m^{-2}. The sawtooth crash is assumed to occur at t=0.

The simulation is performed starting from a standard prescription for the initial temperature perturbation profile: T_{e0} is flattened out to the mixing radius, here taken to be $r_{mix}=0.29$ m. Energy conserving instantaneous reconnection gives an inversion radius value of $r_{inv}=0.18$ m. As a boundary condition, $\tilde{T}_e$ is assumed to vanish at r=a=1 m.

The choice of equilibrium parameters for the simulation of Fig.1 is grossly reminiscent of typical JET plasma parameters, without aiming at reproducing any particular JET discharge. For the perturbation, the parameters of a simulation of a TFTR ballistic heat

pulse have been used [2]. This model need not be at all applicable to JET heat pulses. In particular, due to the low value of χ_e^p assumed, the heat pulses of Fig.1 are rather long, especially in the outer region of the plasma where the time-to-peak exceeds 50 ms. This would not have been the case if standard enhancement of χ_e^p over χ_e^{PB} had been used. The purpose of the simulation is simply to provide an example of ballistic heat pulse on which to illustrate the use of Fourier analysis.

3. Fourier analysis of a ballistic heat pulse

Fourier analysis of the simulated heat pulse is performed using the procedure of Ref.[4] to which we refer for details. Before the analysis, all data are multiplied by a damping function $\exp(-t/\theta)$ with θ=15 ms. This is to ensure that the perturbation vanishes at t=100 ms, which is the end time of the simulation. Multiplication by a damping function was shown in [4] to have a negligible effect on the results for not too small values of θ.

The quantities of interest to be determined with the Fourier analysis are the gradient of the phase (φ') and the logarithmic gradient of the amplitude (A'/A) of the Fourier transform $T_\omega=Ae^{i\varphi}$ of $\tilde{T}_e$. For a purely diffusive heat pulse in cylindrical geometry with negligible damping and not too large gradient of χ_e^p, the following relation between φ' and A'/A holds [4,6]:

$$\varphi'=(A'/A)_g \qquad (12)$$

where $(A'/A)_g=A'/A+1/2r-1/2r_n$ includes some (geometrical) corrections to A'/A; $r_n=-(n_{e0}'/n_{e0})^{-1}$ is the scale length of the density gradient. Note that both φ' and A'/A are negative for an outward propagating heat pulse.

Under the same conditions, the value of χ_e^p is determined from the following expression

$$\chi_g^p=\frac{3}{4}\omega\left[\varphi'\left(\frac{A'}{A}\right)_g\right]^{-1} \qquad (13)$$

The Fourier analysis represents an unambiguous method to establish the diffusive nature of a heat pulse. Non-diffusive features will show up in the analysis in the form of a

difference between φ' and $(A'/A)_g$ at all frequencies. Only if $\varphi'=(A'/A)_g$ do we expect Eq.13 to provide the correct numerical value for χ_e^P. An exception would be the presence of strong damping of the pulse, in which case Eq.13 is still valid even if φ' and $(A'/A)_g$ are different [6].

The results of the Fourier analysis of the ballistic simulation of Fig.1 are shown in Fig.2 for the frequency range $10 \leq \omega/2\pi \leq 30$ Hz. At r=0.5m, the pulse is still strongly influenced by the ballistic effect: φ' is nearly independent of frequency and is significantly lower than $(A'/A)_g$. A saturation of φ' is a typical feature of the heat source term in Eq.6 due to the ballistic enhancement of the diffusivity; the effect on A'/A is smaller. Application of Eq.13 to determine χ_e^P results in an error of a factor 2-3. At r=0.6 m, the comparison between φ' and $(A'/A)_g$ still shows a significant difference between the two quantities, although Eq.13 determines χ_e^P with an error of only 10-30% in this case. In order to observe a purely diffusive behaviour of the pulse, one has to go as far as r=0.7 m. There the agreement between φ' and $(A'/A)_g$ is very good, and the error in the determination of χ_e^P is very small except for the lowest frequency $\omega/2\pi=10$ Hz, where the effect of the boundary condition starts to be significant. Clearly, the ballistic effect is quite strong in this simulation: despite the mixing radius is $r_{mix}=0.29$ m, one has to go to $r>2r_{mix}$ in this particular example before the heat pulse can be regarded as purely diffusive. At these radii, the amplitude of the heat pulse is rather small (below 50 eV in this simulation). Other combinations of parameters in the simulation will result in more or less favourable conditions for diffusive propagation. The point made here is that if a diffusive region exists, it can be recognised by Fourier analysis. Note that this is very different from performing a best fit to the data by assuming a diffusive model. As shown in [2], simulations made under very different assumptions can result in time traces that are not too dissimilar at first sight; their Fourier spectrum, however, is significantly different. This can be understood since Fourier analysis is very sensitive to the rise phase of the pulse, which is different for a diffusive or ballistic pulse. Of course the possibility for the Fourier analysis to recognise a diffusive pulse is ultimatey limited by the s/n ratio of the measurement. This must be judged from case to case when doing the analysis of experimental data.

Even if the pulse of Fig.1 is diffusive for $r>2\ r_{mix}$, application of the extended time-to-peak (E-ttp) method [7] yields a χ_e^P value that is about 30% too large. This kind of shortcoming is common to all methods of analysis based on the standard model for the sawtooth initial perturbation, which is not applicable to a strongly ballistic sawtooth crash [2].

4. A practical definition of r_{mix}

The fact that the ballistic behaviour of a heat pulse must disappear at sufficienty large radii is trivial and was pointed out already in [8]. The Fourier method provides a rigorous approach for determining the boundary outside which diffusive analysis is applicable (with some systematic error depending on the analysis method). However, Fourier analysis is not always accurate enough depending on the s/n level in the data. This was the case, for instance, for many of the heat pulses recorded at JET with the ECE polychromator diagnostic [7]. In cases where Fourier analysis is not possible, other approaches must be used in order to recognise the diffusive region of the pulse. A possible approach is to study the initial perturbation of the pulse.

In Fig.3, the temperature perturbation profile for the simulation of Fig.1 is shown at t=0.5 ms and t=1 ms (at t=0, the perturbation vanishes outside r_{mix}). One can see that within 1 ms of the sawtooth crash, the perturbation has extended over a region well beyond r_{mix} as a result of the ballistic enhancement of the diffusivity. There is no sharp boundary for this extended perturbation, but in practice one can see that the perturbation is negligibly small for r>0.6-0.7 m, both at t=0.5 ms and t=1 ms. Now $r\approx$0.6-0.7 m is just where the heat pulse starts to be diffusive according to Fourier analysis. On the basis of this simple observation, one can therefore justify the approach used, for instance, in previous analyses of JET sawtooth heat pulses [9]. These heat pulses were diagnosed with a typical time resolution of 0.5-1 ms, which prevented an accurate determination of r_{mix}. Nevertheless, r_{mix} was defined heuristically as the radius beyond which the initial perturbation vanished, and the heat pulse analysis was carried out for $r>r_{mix}$. Applying this approach to our simulation, taking into

account the diagnostic delay time of about 1 ms, would give a value of $r_{mix} \approx 0.6$ m. Thus, even without doing any Fourier analysis, one can perform the heat pulse analysis having minimised the errors due to the ballistic component of the heat pulse.

The main weakness in this approach is the lack of knowledge on the time scale of the ballistic effect. In our example, τ_b coincides roughly with the time resolution of the diagnostic. In a real case, longer values of τ_b cannot be excluded. One should then study the time evolution of the pulse in its early phase to see if the propagation is diffusive or not. This is where Fourier analysis is essential. An alternative approach, not discussed here, is to use analysis techniques that can be extended into the region of the initial perturbation, such as the double forced boundary method used in [10]. In that case, the time interval where the ballistic enhancement occurs can be excluded from the analysis.

5. Fourier analysis of a JET heat pulse

It is interesting to compare the results of the simulation with a recent example of JET sawtooth heat pulse diagnosed with the new ECE heterodyne diagnostic. This diagnostic covers most of the electron temperature profile with a spatial resolution of about 3 cm. The noise level depends on the electrical bandwidth: for typical heat pulse signals (1 kHz electrical bandwidth), the noise equivalent temperature is 10 eV (standard deviation). An example of sawtooth heat pulse measured with the ECE diagnostic is shown in Fig.4. This example is a good illustration of the s/n level of the diagnostic. The space resolution can be inferred from Fig.5, which shows the temperature profile just before the sawtooth crash and about 200-300 μs afterwards (a) as well as their difference (b). The difference profile has the role of initial perturbation for the heat pulse, in the sense discussed in the previous section. The corresponding normalised mixing radius value is $\rho_{mix} \approx 0.7$; this is more than twice the value of the inversion radius ($\rho_{inv}=0.32$).

Fourier analysis (Fig.6) must be restricted to the region $\rho>0.7$ in order to provide a good determination of χ_e^p. The values of φ' and $(A'/A)_g$ in the region $\rho>0.7$ are plotted vs frequency in Fig.6a. The diffusive behaviour of the heat pulse is demonstrated by the equality

of the φ' and $(A'/A)_g$ values for $\omega/2\pi \geq 30$Hz. At lower frequencies, the difference between φ' and $(A'/A)_g$ is consistent with the estimated damping time value τ=50 ms due to perturbed energy sinks (i.e., electron-ion heat exchange and Ohmic heating). The χ_e^P value determined from the data of Fig.6a using Eq.13 is χ_e^P=3.5 m^2/s. A similar value of χ_e^P=3.0 m^2/s is obtained with the E-ttp method. It is interesting to see what would be the consequence of including data with $\rho<\rho_{mix}$ in the analysis. This is shown in Fig.6b, where the values of φ' and $(A'/A)_g$ in the region $\rho>0.6$ (7 channels) are plotted. The values of φ' are seen to be significantly smaller than their true value, while the value of $(A'/A)_g$ has remained unchanged. This result is similar to the analysis of the ballistic heat pulse shown in Fig.3. Given the time resolution of the diagnostic, however, it is not possible to decide whether the heat redistribution causing the large r_{mix} value occurs on a fast (τ_{ST}) time scale or on a slower (ballistic) time scale.

The large ρ_{mix} value of this heat pulse prevents a meaningful comparison between perturbed (χ_e^P) and power balance (χ_e^{PB}) diffusivity values due to the large uncertainties in χ_e^{PB} near the plasma edge. Other sawtooth heat pulses measured with the heterodyne diagnostic have smaller ρ_{mix} values and confirm the result $\chi_e^P/\chi_e^{PB} \approx 2$-4 typical of JET plasmas.

As a final comment, it seems to us that the ballistic effect is an interesting property of the sawtooth crash that deserves further investigation. For instance, it may help understand the relation between transport and magnetic turbulence. The consequences of the ballistic effect on the subsequent heat pulse propagation can normally be recognised and do not prevent an accurate determinaton of χ_e^P. While a detailed investigation of the ballistic pulse requires a very good time resolution, indirect evidence of the effect can be sought with moderate time resolution diagnostics by studying the profile of the initial temperature perturbation. This will be the subject of future work.

6. Conclusions

Application to a simulated ballistic sawtooth heat pulse has shown that Fourier analysis can identify the plasma region (far from the mixing radius) where the heat pulse is diffusive. This region coincides with the region where a diagnostic with moderate (≈1 kHz) time resolution woud find a negligible initial perturbation. Fourier analysis of an example of JET sawtooth heat pulse diagnosed with the new ECE heterodyne diagnostic and showing a broad initial perturbation is consistent with the results of simulated data. While a detailed investigation of the ballistic pulse requires a very good time resolution, it may be possible to find indirect evidence of the effect in tokamaks other than TFTR by studying the shape of the initial temperature perturbation profile. In cases where the initial perturbations of the JET sawtooth heat pulses are not very broad, comparison between perturbed (χ_e^P) and power balance (χ_e^{PB}) diffusivity values confirms the result $\chi_e^P/\chi_e^{PB}\approx$2-4 typical of JET plasmas.

Acknowledgement

Useful discussions with V.Parail, A.C.C.Sips and A.Taroni are gratefully acknowledged.
This work was performed under the JET-ENEA-CNR task agreement on perturbative transport, with financial support from JET and CNR.

References

[1] N.J.Lopes Cardozo, Perturbative Transport Studies in Fusion Plasmas, to appear in Plasma Phys. Contr. Fusion (1995).

[2] E.D.Fredrickson et al, Phys. Rev. Lett. 65 (1990) 2869; E.D.Fredrickson et al, Nucl. Fusion 33 (1993) 1759.

[3] A.Krämer-Flecken, G.Waidmann, in Controlled Fusion and Plasma Physics (Proc. 21st Eur Conf Montpellier, 1995), Vol 18B, Part I, European Physical Society, Geneva (1995) 122.

[4] P.Mantica et al, Nucl. Fusion 32 (1992) 2203.

[5] K.W.Gentle et al, An Experimental Counter-Example to the Local Transport Paradigm, to appear in Physics of Plasmas (1995).

[6] A.Jacchia et al, Phys. Fluids B 3, 3033 (1991).

[7] B.J.D.Tubbing et al, Nucl. Fusion 27, 1843 (1987).

[8] A.C.C.Sips et al, in Controlled Fusion and Plasma Physics (Proc. 18th Eur Conf Berlin, 1991), Vol 15C, Part I, European Physical Society, Geneva (1991) 193.

[9] N.J.Lopes Cardozo, A.C.C.Sips, Plasma Phys Contr Fusion 33 (1991) 1337.

[10] S.V.Neudatchin, D.G.Muir, The Study of Electron Heat Transport in JET Analysing the Decay of Temperature Perturbations induced by Sawteeth, Rep. JET-P(93)27, JET Joint Undertaking, Abingdon, UK (1993).

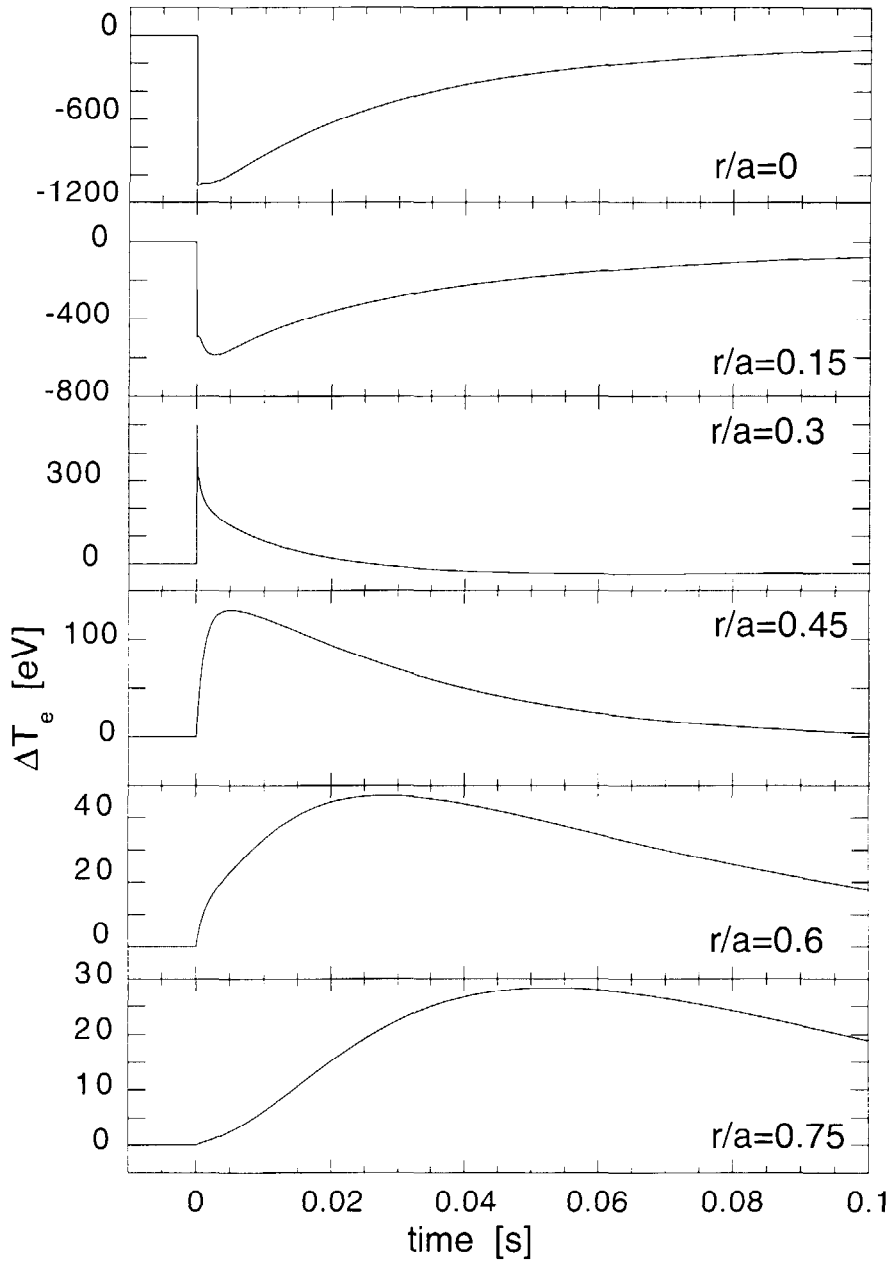

1. Example of simulated ballistic sawtooth heat pulse. Shown is the time evolution of the temperature perturbation at several radial locations in the plasma.

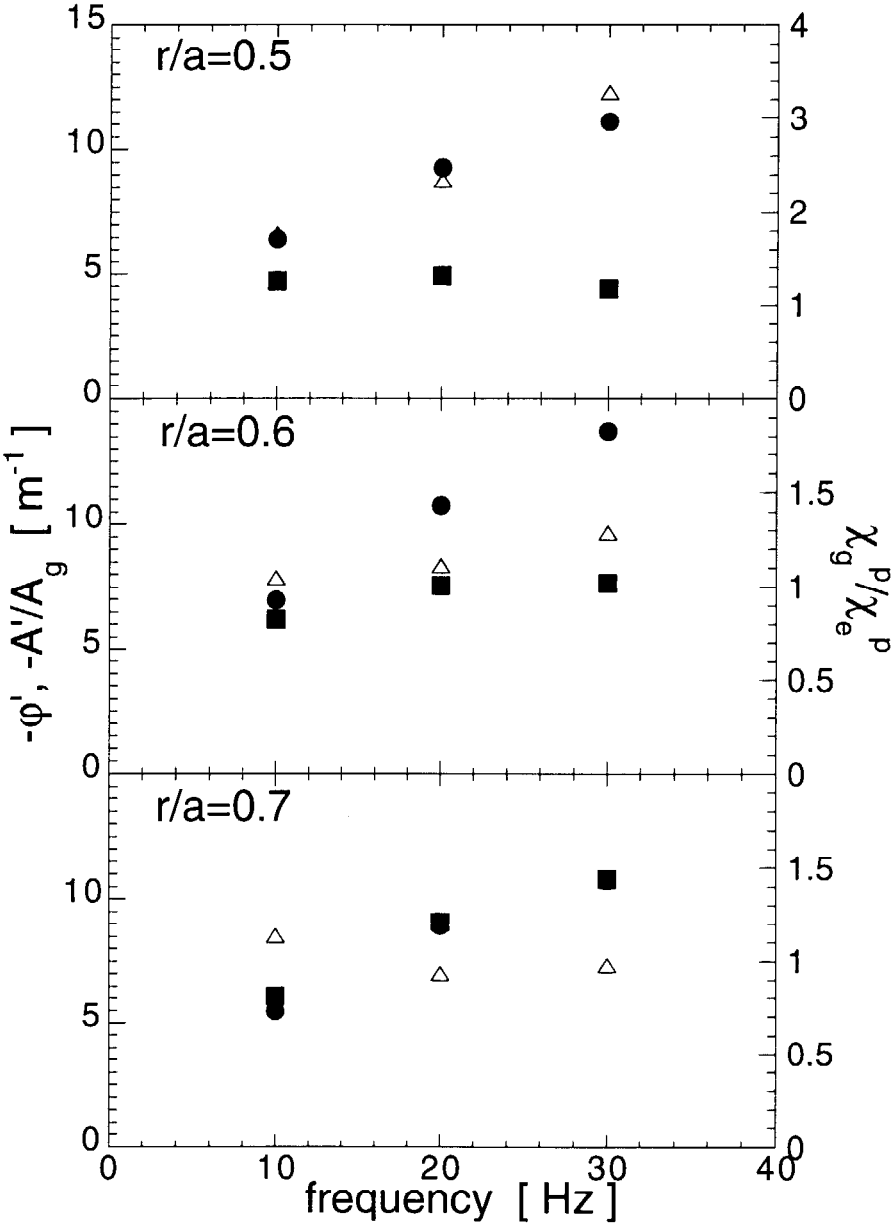

2. Values of φ' (squares) and $(\Lambda'/\Lambda)_g$ (circles) obtained from the simulated heat pulse of Fig.1 at three different locations in the plasma, plotted vs frequency. The χ_{eg} value from Eq.13 (open triangles) normalised too the true χ_e^p vaue is also shown on the same plots.

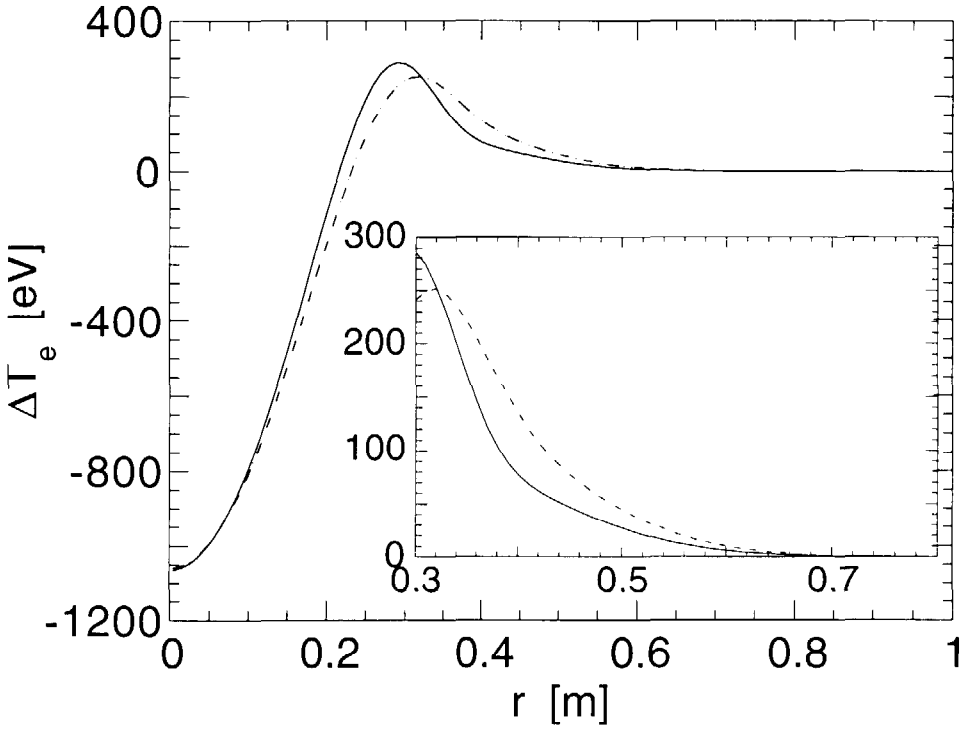

3. Spatial profile of the electron temperature perturbation for the simulated heat pulse of Fig.1 for t=0.5 ms (full line) and t=1 ms (dashed line). The same profiles are plotted in the insert over the radial range 0.3<r<0.8.

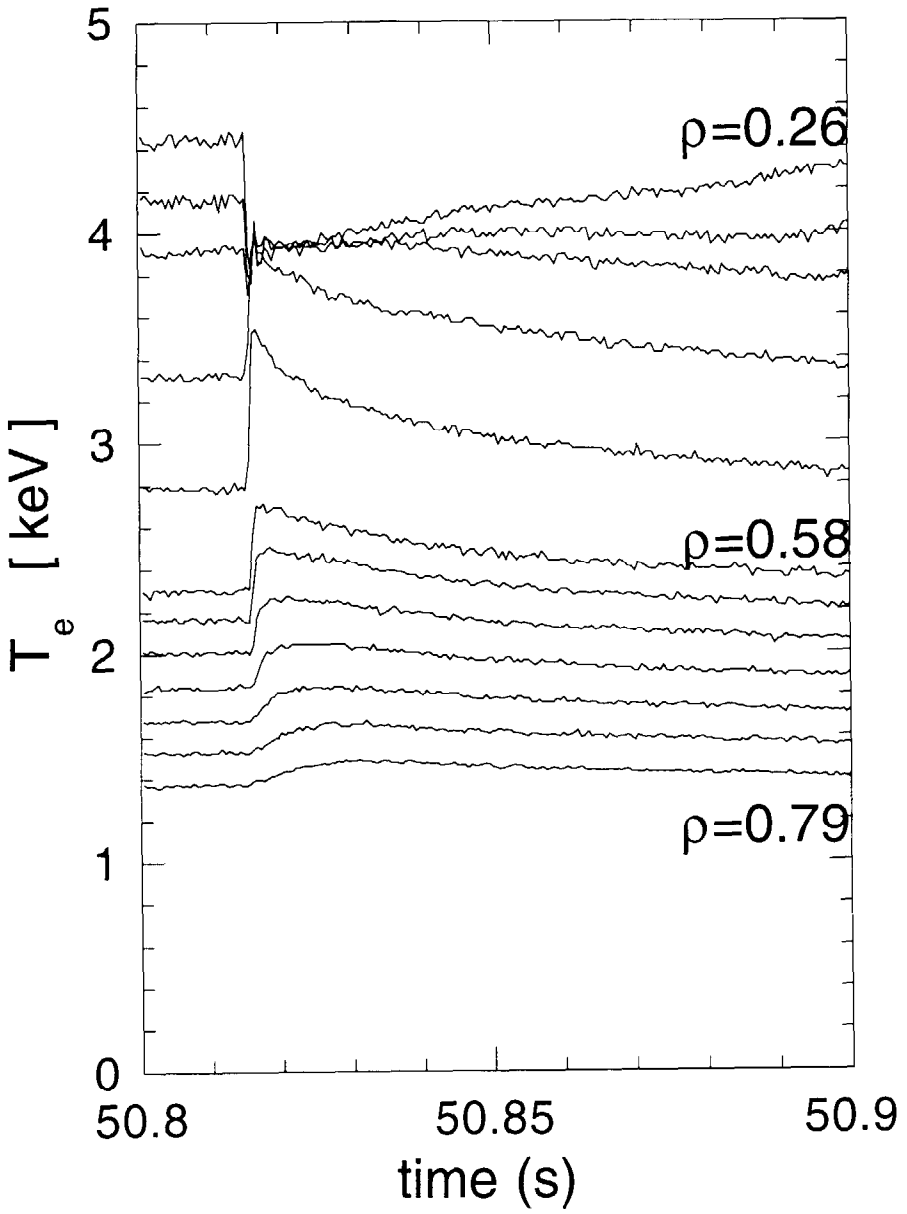

4. Time evolution of the electron temperature following a sawtooth instabilty in JET discharge #23425 as recorded by the ECE heterodyne diagnostic (time resolution Δt=0.5 ms) at selected radial locations. This was a discharge with B=3.4 T, I_p=3.5 MA, $\langle n_e \rangle = 1.4 \cdot 10^{19}$ m^{-3}, $\langle T_e \rangle$=2 keV, P_{OH}=1.5 MW, P_{RF}=3.8 MW, horizontal minor radius a=1.11 m. The sawtooth instability occurs at t=50.815 s.

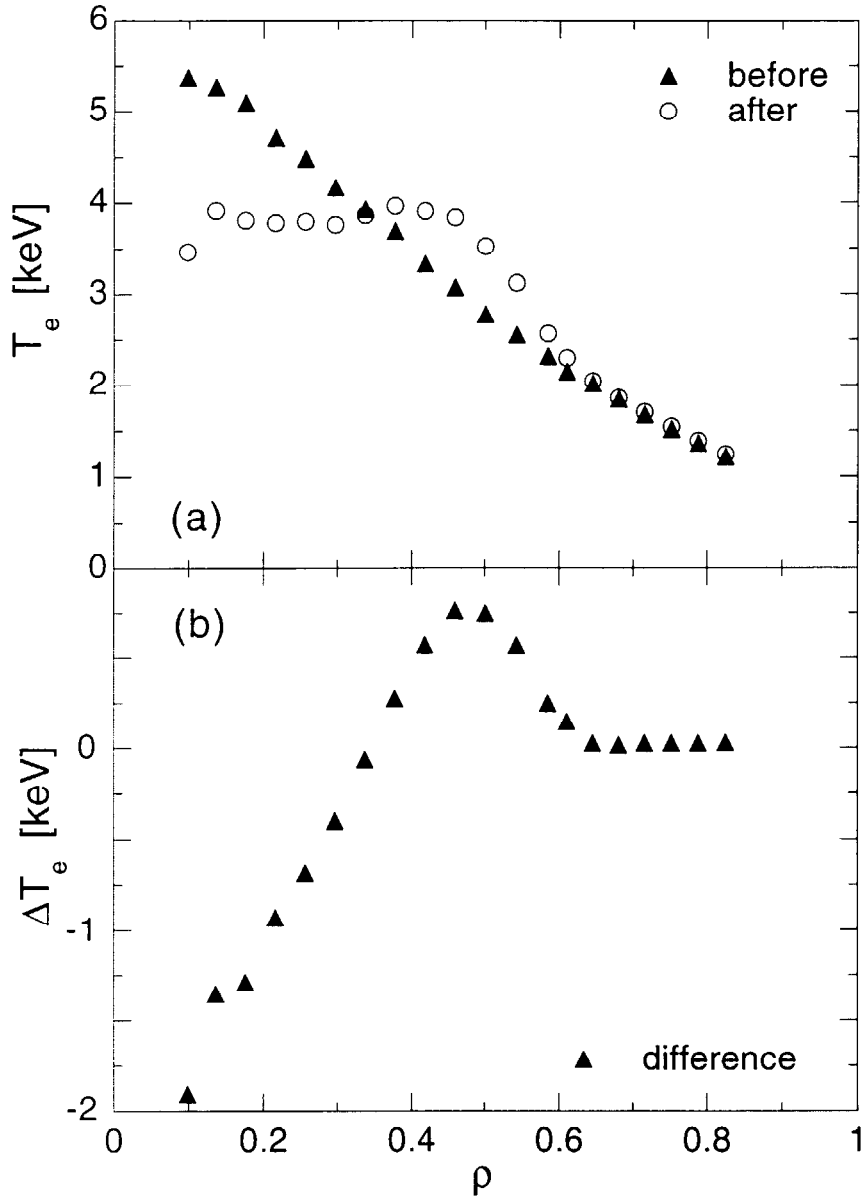

5. Change in the electron temperature profile due to the sawtooth instability of Fig.4. The T_e profile perturbation extends out to $\rho \approx 0.6$-0.7.

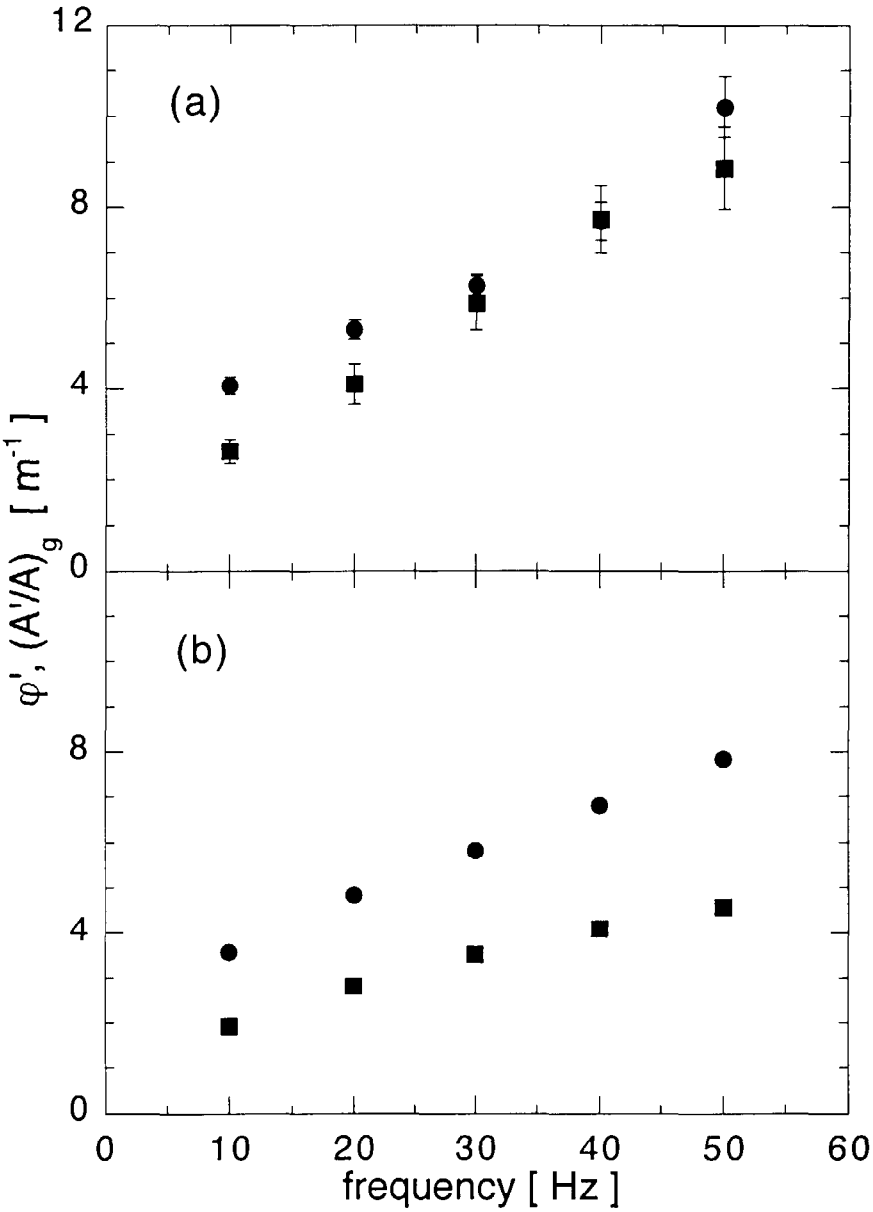

6. Values of φ' (squares) and $(A'/A)_g$ (circles) from the sawtooth heat pulse of Fig.4. The derivatives are calculated over (a) the 4 outermost ECE channels ($0.7<\rho<0.85$) and (b) the 7 outermost ECE channels ($0.6<\rho<0.85$). The statistical error bars shown in (a) were determined from the noise level of the data using the method of Ref.[4]. The error bars in (b) are comparable to the size of the symbols.